

## Research Article

# Study on Quantitative Phase Imaging by Dual-Wavelength Digital Holography Microscopy

Lin Hu, Yunxiu Shui, Yaohui Dai, Haiyu Wu, Gang Zhu, and Yan Yang 

College of Mechanical Engineering, Chongqing University of Technology, Chongqing 400054, China

Correspondence should be addressed to Yan Yang; yangyan@cqut.edu.cn

Received 15 October 2018; Revised 18 October 2018; Accepted 21 October 2018; Published 1 November 2018

Guest Editor: Xiaowei Li

Copyright © 2018 Lin Hu et al. This is an open access article distributed under the Creative Commons Attribution License, which permits unrestricted use, distribution, and reproduction in any medium, provided the original work is properly cited.

A dual-wavelength digital holographic microscopy with premagnification is proposed to obtain the object surface measurements over the large gradient. The quantitative phase images of specimens are captured in high precision by the processing of filtering and phase compensation. The phase images are acquired without phase unwrapping, which is necessary in traditional digital holographic microscopy; thereby the proposed system can greatly increase the speed of reconstruction. The results of numerical simulation and optical experiments demonstrated that the reconstructed speed increased by 37.9 times, and the relative error of measurement is 4% compared with the traditional holographic microscopy system. It means that the proposed system can directly acquire the higher quality quantitative phase distribution for specimens.

## 1. Introduction

Digital holographic microscopy (DHM) is a powerful technology for the measurement of microscopic samples by recording and reconstructing the amplitude and phase of the wave. The dual-wavelength digital holographic microscopy uses two different wavelength lasers to simultaneously record the hologram and numerically reconstruct the phase information according to phase distribution under two wavelengths. As early as 1998, a new method for the extraction of quantitative phase imaging by using partially coherent illumination and an ordinary transmission microscope was proposed by A. Barty et al., which can recover a phase even in the presence of amplitude modulation [1]. A solution for absolute phase measurements was presented by Cuhe Etienne et al. [2]. They introduced digital reference wave and phase mask, which were applied in phase-contrast imaging and optical metrology. This property of holograms offers phase-contrast techniques, which can be used in quantitative 3D imaging. The compensation of the inherent wave front curvature by subtracting the reference hologram in DHM for quantitative phase-contrast imaging is introduced by Ferraro, Pietro, et al. [3]. This simple method can be implemented efficiently under the ideal experimental conditions. The dual-wavelength phase-shifting digital holography that selectively

extracts wavelength information from five wavelength-multiplexed holograms is presented by Tahara, Tatsuki, et al. [4]. The color hyperchaotic image encryption method by the DHM and CA encoding algorithm is proposed by Sichuan University, which has great security and robustness [5, 6]. It is an important application about digital holography. The enhanced quantitative three-dimensional measurement system is introduced by JaeYong Lee. It can simplify the configuration by a dual-peak quantum dot wavelength converter and a blue LED [7]. There are great researches for reducing speckle noise and increasing the speed of reconstruction [8–10]. We have successfully achieved the near real-time three-dimensional surface measurement by digital holography [11, 12].

If the optical path difference is less than the equivalent wavelength, the real phase distribution of object can be directly obtained without phase unwrapping by the dual-wavelength digital holographic interferometry. If the optical path difference is greater than the equivalent wavelength, the phase unwrapping process will be simplified by dual-wavelength digital holographic interferometry. The noise immunity and the scope of phase unwrapping algorithms will be improved and expanded, respectively [13–15]. C. J. Mann obtained the measurement results of the surface height over several microns of range by three-wavelength digital

holography [16]. The optical path length can be converted to physical thickness, and the sample height information will be provided. The dual-wavelength DHM imaging experiment of a stepped phase plate and the smoke particles were conducted by P. Song et al. [17]. M.K. Kim et al. successfully achieved three-dimensional imaging of resolution plates and cancer cells using dual-wavelength DHM [18]. A phase-imaging technique to quantitatively study the three-dimensional structure of cells by simultaneous dual-wavelength reflection digital holography was presented by A. Khmaladze et al. [19]. It proves that the dual-wavelength DHM allows a faster imaging, which does not rely on the surrounding pixels to correct the phase discontinuities, but simply compares two single-wavelength phases. Dual-wavelength DHM has been widely applied in the fields of surface topography measurement [20–22], cell imaging [23, 24], 3D particle imaging [25, 26], transparent medium physical quantity measurement [27–29], and so on. Due to the limitation of the dual-wavelength DHM technique, more noise will be introduced with the increase in synthesis wavelength and the expanding of the sample range. The accuracy of measurement decreased as the noise increased. The setup of dual-wavelength DHM consists of two laser machines, which makes it difficult to ensure the concentricity of two laser beams in an optical assembly. All the above have the adverse effects on obtaining high precision phase information.

A system of dual-wavelength DHM with premagnification, which can directly and accurately obtain quantitative phase images, is presented. The principle of surface topography measurement and phase unwrapping method based on dual wavelength digital holography is introduced. The effectiveness of the system is verified by computer simulations and optical experiments using the 1951 USAF target and the standard groove object. Compared with the traditional single wavelength DHM, the system can not only obtain the phase information without phase unwrapping, but also get the low noise and high precision quantitative phase images.

## 2. Experimental Principle

**2.1. Principle.** In dual-wavelength digital holographic microscopy, two laser beams in different wavelengths from separated laser sources are coupled into one beam, and the optical assemblies are shown in Figure 1. The two lasers were used as coherent light sources. Both beams are collimated by spatial filter. Beam splitters (BS1) divide the beams into the reference and the object arms. The object beam passes through the sample and microscope objective. There are different tilts in orthogonal directions for reference waves of two lasers, which allows us to capture both wavelengths simultaneously. Then the interference pattern between the reference waves and object wave is recorded by a CCD camera.

The dual-wavelength composite digital hologram will be acquired on the CCD, and the interference pattern can be expressed as

$$I_H(x, y) = |O_1|^2 + |R_1|^2 + |O_2|^2 + |R_2|^2 + R_1^* O_1 + R_1 O_1^* + R_2^* O_2 + R_2 O_2^* \quad (1)$$

where  $I_H$  is the intensity of the composite digital hologram,  $x, y$  are the coordinates of the holographic plane,  $*$  is the complex conjugate,  $O_1, O_2$  are object beams, and  $R_1, R_2$  are reference beams.

The interferometric phase can be extracted by the spatial filtering method and shifted to the center position to perform the Fourier transform. The complex amplitude distribution of the reproducing light field can be obtained as follows:

$$O_i(x, y) = R_i(x, y) [R_i^*(x, y) O_i(x, y)] \quad i = 1, 2 \quad (2)$$

The intensity and the wavefront phase distribution of optical field can be calculated according to the following expressions:

$$I_i(x, y) = O_i(x', y') R_i^*(x', y') \quad (3)$$

$$\Phi_i(x, y) = \arctan \left[ \frac{\text{Im} O_i(x', y')}{\text{Re} O_i(x', y')} \right] \quad (4)$$

In order to overcome the issue of phase ambiguity produced by single wavelength approach, a synthetic beat-wavelength is used and expressed as follows:

$$\Phi = \Phi_1(x, y) - \Phi_2(x, y) = 2\pi \frac{nh}{\lambda_1} - 2\pi \frac{nh}{\lambda_2} = 2\pi \frac{nh}{\Lambda} \quad (5)$$

where  $h$  is the height distribution of the specimens, which means the optical path difference of the twice of the topography for reflection scheme.  $nh$  is the optical path difference of the homogeneous sample in the air.  $\Lambda$  is the equivalent wavelength defined as follows:

$$\Lambda = \frac{\lambda_1 \lambda_2}{|\lambda_1 - \lambda_2|} \quad (6)$$

If the optical path difference is less than the equivalent wavelength, the real phase of specimens can be directly obtained without unwrapping. Otherwise, the phase distribution is wrapped between  $-\pi$  and  $+\pi$ . In this case, the package phase difference is compensated to obtain its equivalent phase.

$$\Phi \begin{cases} \Phi_1(x, y) - \Phi_2(x, y) & \Phi > 0 \\ \Phi_1(x, y) - \Phi_2(x, y) + 2\pi & \Phi < 0 \end{cases} \quad (7)$$

In summary, the dual-wavelength digital holographic microscopy to measure the large gradient of specimens can solve the problem of phase unwrapping with single-wavelength digital holographic microscopy. As the range of measurement increases, the noise of the phase distribution in the single-wavelength digital holographic microscope also increases. Therefore, the reasonable choice of wavelength and the method of noise reduction are key points in the dual-wavelength holographic microscopy.

## 3. Experimental Results

**3.1. Experimental Setup.** The experiments were conducted in a DHM developed by our team. The schematic diagram and

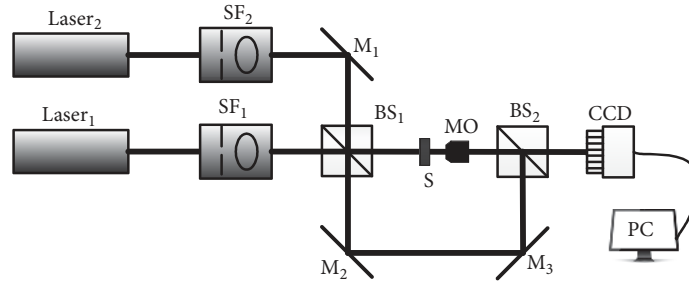


FIGURE 1: The schematic diagram of dual-wavelength digital holographic microscopy. SF, spatial filter; M, mirrors; BS, beam splitters; S, sample; MO, microscope objective; CCD, charge-coupled devices; PC, personal computer.

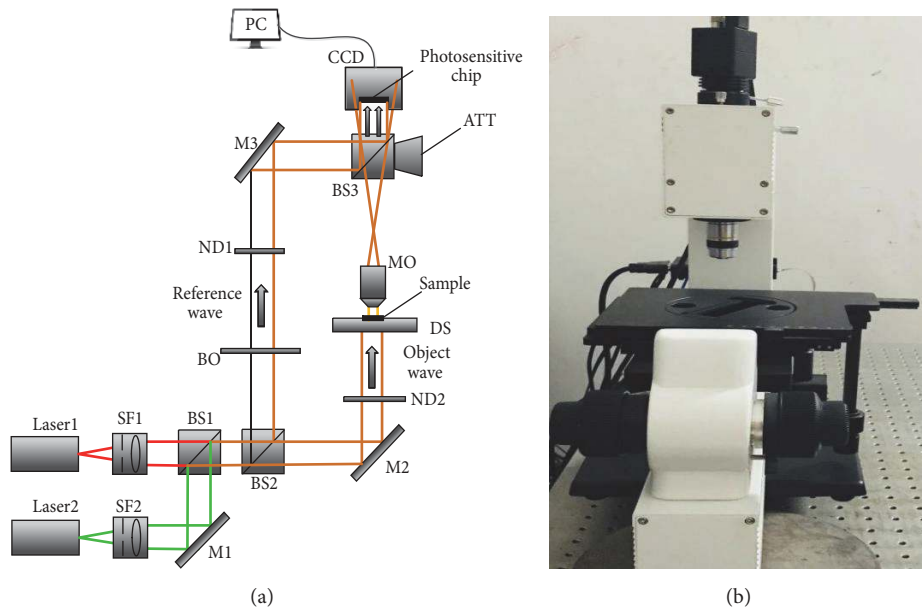


FIGURE 2: (a) The schematic diagram of the dual-wavelength DHM system. SF, spatial filter; BS, beam splitters; M, mirrors; ND, neutral density; DS, displacement stage; S, sample; MO, microscope objective; ATT, adjustable tilting stage; BO, beam obstacle. (b) Real picture of DHM.

the setup are shown in Figure 2, where  $\lambda_1 = 632.8 \text{ nm}$  and  $\lambda_2 = 532 \text{ nm}$ , the equivalent wavelength,  $\Lambda = 3.34 \mu\text{m}$ . The beams emitted by the two lasers pass through the beam expanders and collimation systems (SF), the mirror and the cube beam splitter (BS). Then the beam is divided into two beams by beam splitter; one is object wave, and the other is the reference wave. In the preamplification optical path, the object wave, which is reflected by mirror, passes through the microscope objective (MO,  $10\times$ ,  $NA = 0.25$ ) and the sample. On the other hand, the reference wave passes through beam obstacle and neutral density. It should be noted that beam obstacle is turned on so that the optical path is the one of off-axis digital holography (in this experiment, the beam obstacle is turned on); otherwise, it will become in-line digital holography. The two beams are combined by the cube splitting prism. Finally, the interference hologram is recorded by CCD (SENTECH STC-SBS241POE; the pixel area is  $1296 \text{ pixel} \times 966 \text{ pixel}$ ). It is worth noting that the dual-wavelength preamplification digital holographic microscopy systems with large numerical aperture microscope objectives

can acquire more sample information, which can be compressed to amplify the CCD acceptable sampling frequency [30].

**3.2. Numerical Simulation.** In order to illustrate that the phase image of sample whose optical path difference is less than the equivalent wavelength can be obtained directly and quickly by dual-wavelength DHM; a numerical simulation experiment is carried out. The computer-generated cone is a phase object with a maximum phase height of  $2.5 \mu\text{m}$ . The simulation parameters of cone are as follows:  $\lambda_1 = 632.8 \text{ nm}$ ,  $\lambda_2 = 532 \text{ nm}$ , in which each single wavelength is less than the optical path difference. According to (6), the equivalent wavelength is  $3.34 \mu\text{m}$ , which means that the dual-wavelength phase unwrapping will obtain a continuous phase distribution. Based on the designed height, the wrapping phase distribution of single-wavelength and the phase distribution of equivalent wavelength are shown in Figure 3, respectively.

To demonstrate the advantages and compare the unwrapping speed of the dual-wavelength DHM and traditional

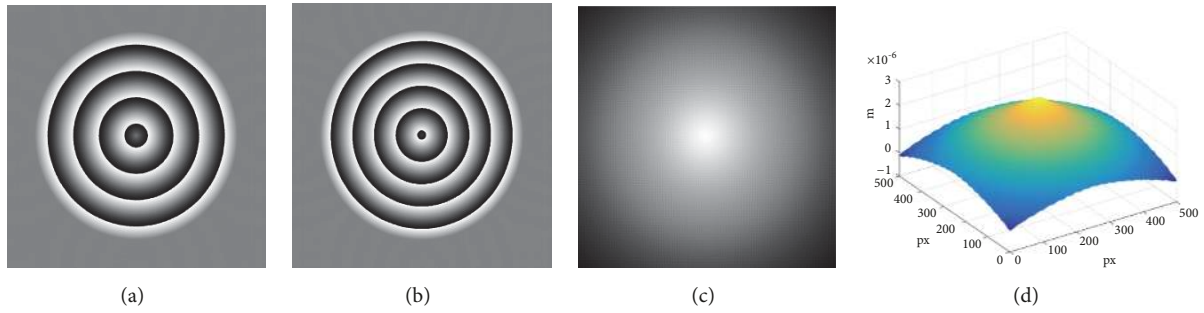


FIGURE 3: Simulation results for slope: (a) phase distribution for  $632.8 \text{ nm}$ , (b) phase distribution for  $532 \text{ nm}$ , (c) phase distribution for equivalent wavelength, and (d) 3D view of dual-wavelength phase distribution.

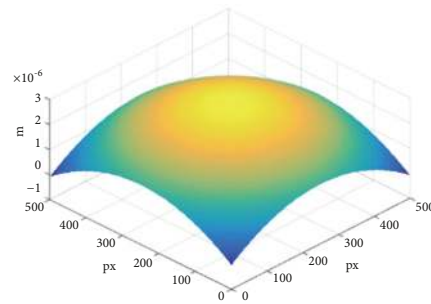


FIGURE 4: 3D view of dual-wavelength phase distribution.

single-wavelength DHM, a  $632.8 \text{ nm}$  wrapped phase image is chosen to obtain the final height distribution by unwrapping procedure, which is named the quality-guided phase unwrapping algorithm. And the results for  $632.8 \text{ nm}$  through the quality-guided phase unwrapping algorithm [31, 32] are shown in Figure 4.

The height distributions of cone by dual-wavelength DHM and quality-guided phase unwrapping method are compared. And the results are shown in Table 1. The results show that both of them can accurately obtain the height distribution of the cone, but in terms of time, the dual-wavelength holographic microscopy in the system is faster. The speed of reconstruction by the proposed system is 37.9 times more than the value of the quality-guided phase unwrapping method.

### 3.3. Optical Experiment

**3.3.1. Quantitative Phase Imaging of USAF 1951 Target.** Based on the dual-wavelength phase imaging system, the surface of an USAF 1951 target was measured. At the same time, the target was also measured by the scanning three-dimensional profiler (NanoMap 500LS, AEP Technology Inc., USA) and the results showed that the height was about  $0 \sim 100 \text{ nm}$ . Since the sample height is much smaller than the single-wavelength, the phase distribution of the sample can be obtained directly. Figures 5 and 6 present the measurement results using traditional single-wavelength and dual-wavelength, respectively.

In the reconstruction process, filtering and secondary phase distortion compensation processing are performed

[33–35]. The hologram is spectrally separated by Fourier transform. The microscope objective lens will introduce a secondary phase distortion factor in the system. In order to obtain the real phase, two holograms are recorded, which are the reference holograms for the background of the hologram and the hologram of measured sample. The real phase can be obtained by subtracting the two reconstruction phases of hologram.

The comparison of the height distribution curve along the middle symmetrical line of phase with different wavelength (in Figures 5(a), 5(b), and 6(a)) is shown in Figure 7. The height distribution along the middle symmetrical line of sample was scanned by NanoMap 500LS and its absolute height was measured to be  $54 \text{ nm}$ . The average absolute height and the relative error between the measurement result and scanning result using three measurement methods are shown in Table 2.

Table 2 shows that the result of the equivalent wavelength is much closer to scanning value. From the experimental results, it can be seen that both the traditional DHM and the dual-wavelength DHM can obtain the phase distribution of the object surface. It is not hard to see that the system of dual-wavelength DHM can accurately obtain the three-dimensional morphology distribution of the object surface. The results prove that the measurement accuracy and stability of the proposed system are better than the traditional single wavelength.

**3.3.2. Quantitative Phase Imaging of Groove.** The transparent groove standard plate, which is artificially designed, was used as an experimental sample to measure its three-dimensional

TABLE 1: Comparison of two methods.

Method	Maximum phase ( $\mu\text{m}$ )	Time (s)
Quality-guided phase unwrapping	2.5749	716.61
Dual-wavelength DHM (in the system)	2.5971	18.93

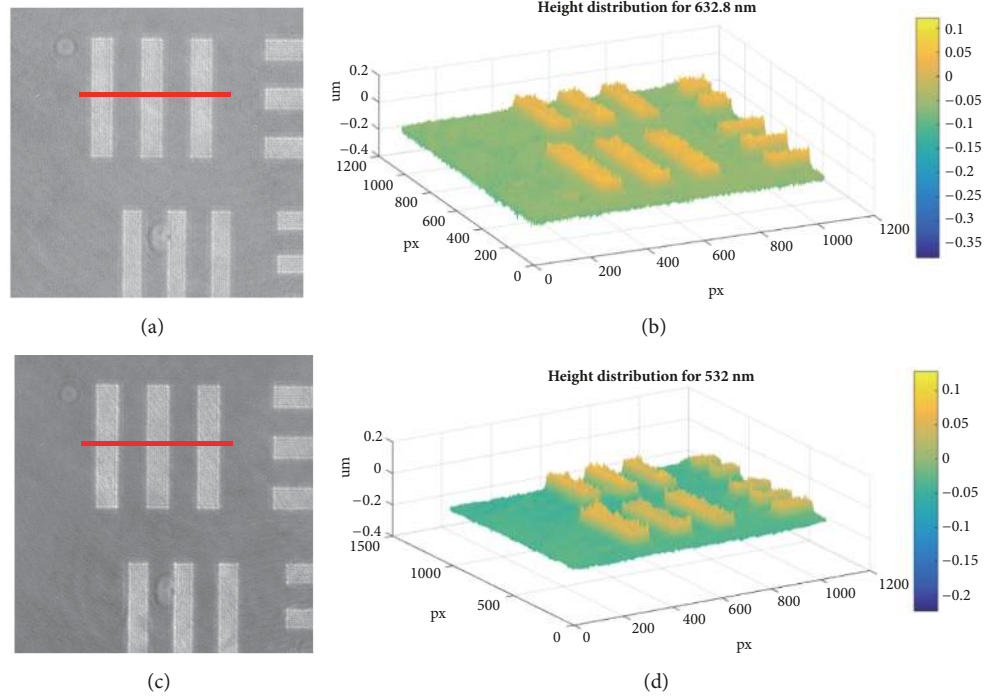


FIGURE 5: Experimental results with single wavelength measurement. (a) Phase image for 632.8 nm, (b) height distribution for 632.8 nm, (c) phase image for 532 nm, and (d) height distribution for 532 nm.

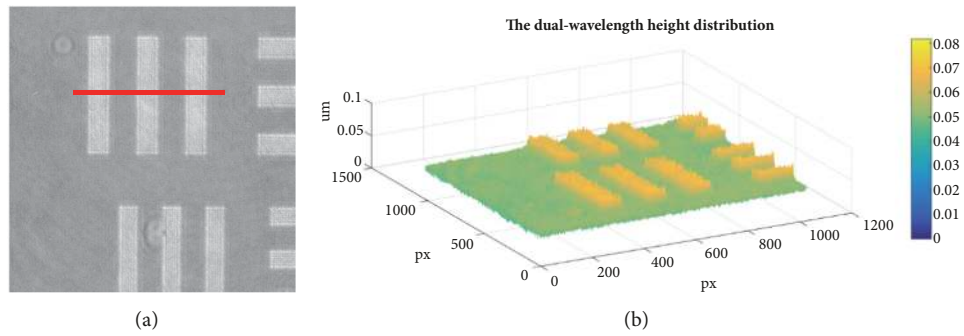


FIGURE 6: Experimental results for equivalent wavelength. (a) Phase image for equivalent wavelength, (b) 3D view of dual-wavelength height distribution.

TABLE 2: The comparison of the height distributions.

Wavelength( nm)	Absolute height ( nm)	Relative error (compared with the scanned value)	Variance
632.8	61.8	14.4%	$1.925 \times 10^{-4}$
532	99.3	83.8%	$3.188 \times 10^{-4}$
equivalent wavelength	47.5	13.8%	$1.504 \times 10^{-5}$

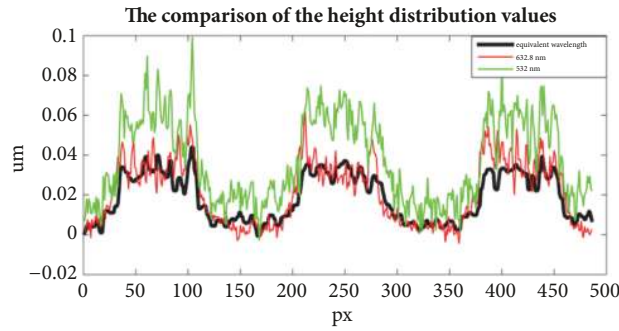


FIGURE 7: The comparison of the height distribution values along the middle symmetrical line of sample in pane Figures 5(a), 5(b), and 6(a).

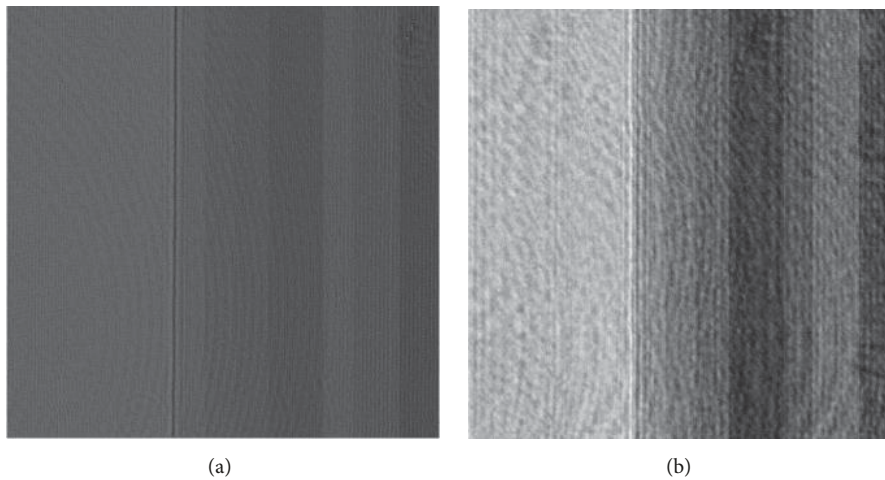


FIGURE 8: Experimental results with single wavelength measurement. (a) Phase image for 632.8 nm, (b) phase image for 532 nm.

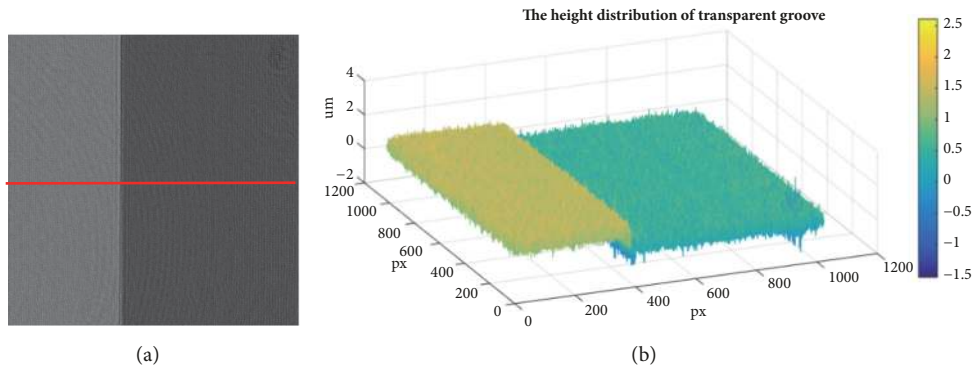


FIGURE 9: Results for equivalent wavelength. (a) Phase distribution, (b) three-dimensional height distribution.

appearance. The width of groove is 1 mm and the depth is 9  $\mu\text{m}$ . Figure 8(a) shows the phase distribution measured by wavelength, 632.8 nm. Figure 8(b) shows the phase distribution measured by wavelength, 532 nm. It is clear to see that there is phase folding in the phase distribution at each single wavelength. The phase distribution measured by the dual wavelength interference is shown in Figure 9.

The height distribution of the middle symmetrical line of the groove (Figure 9(a)) is obtained by the median filtering, which is shown in Figure 10. According to the formula of the surface profile distribution and phase distribution (in (5)),

the height difference between the base and the bottom of the groove  $b = 0.936 \mu\text{m}$ . The relative error between the actual groove height and experimental result is 4%, which is in good agreement with the theoretical values.

#### 4. Conclusions

In order to solve the quantitative phase imaging problem of traditional digital holographic microscopy system for the large gradient of object surface, a dual-wavelength preamplification digital holographic microscopy optical system is

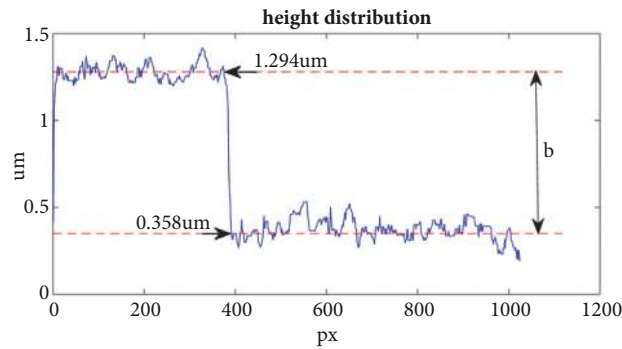


FIGURE 10: Height distribution values along the middle symmetrical line of groove in Figure 8(a).

proposed. The numerical simulation and experiments are carried out and the effectiveness of the system is verified. The experimental results of the sample phase imaging of the traditional DHM and dual-wavelength preamplification DHM system are compared. The results show that the experimental system can effectively overcome the limitations of the single-wavelength method in the imaging of complex surface objects, increase the observation speed, and simplify the reconstruction process, which further validates the effectiveness of the experimental system for quantitative phase imaging.

### Data Availability

The data used to support the findings of this study are included within the article.

### Conflicts of Interest

The authors declare that they have no conflicts of interest.

### Acknowledgments

This work has been supported by the National Natural Science Foundation of China (Nos. 11272368 and 51875068), the International Cooperation Special Project in Science and Technology of China (No. 2015DFR70480), the Chongqing Municipal Education Commission's science and technology research project (KJ1600929), and the Graduate Innovation Foundation of Chongqing University of Technology (No. ycx2018216).

### References

- [1] A. Barty, K. A. Nugent, D. Paganin, and A. Roberts, "Quantitative optical phase microscopy," *Optics Express*, vol. 23, no. 11, pp. 817–819, 1998.
- [2] E. Cucho, F. Bevilacqua, and C. Depeursinge, "Digital holography for quantitative phase-contrast imaging," *Optics Express*, vol. 24, no. 5, pp. 291–293, 1999.
- [3] A. Finizio, C. Magro, G. Pierattini et al., "Compensation of the inherent wave front curvature in digital holographic coherent microscopy for quantitative phase-contrast imaging," *Applied Optics*, vol. 42, no. 11, p. 1938, 2003.
- [4] T. Tahara, R. Mori, S. Kikunaga, Y. Arai, and Y. Takaki, "Dual-wavelength phase-shifting digital holography selectively extracting wavelength information from wavelength-multiplexed holograms," *Optics Express*, vol. 40, no. 12, pp. 2810–2813, 2015.
- [5] X. Li, Y. Wang, and Q. H. Wang, "Modified integral imaging reconstruction and encryption using an improved SR reconstruction algorithm," *Optics & Lasers in Engineering*, pp. 112–162, 2019.
- [6] X. Li, D. Xiao, and Q.-H. Wang, "Error-free holographic frames encryption with CA pixel-permutation encoding algorithm," *Optics and Lasers in Engineering*, vol. 100, pp. 200–207, 2018.
- [7] S. Jeon, J. Lee, J. Cho, S. Jang, Y. Kim, and N. Park, "Wavelength-multiplexed digital holography for quantitative phase measurement using quantum dot film," *Optics Express*, vol. 26, no. 21, p. 27305, 2018.
- [8] H. Cho, D. Kim, Y. Yu, W. Jung, and S. Shin, "Dual-wavelength Digital Holography Microscope for BGA Measurement Using Partial Coherence Sources," *Journal of the Optical Society of Korea*, vol. 15, no. 4, pp. 352–356, 2011.
- [9] J. Cho, J. Lim, S. Jeon et al., "Dual-wavelength off-axis digital holography using a single light-emitting diode," *Optics Express*, vol. 26, no. 2, pp. 2123–2131, 2018.
- [10] V. Bianco, P. Memmolo, and M. Leo, "Strategies for reducing speckle noise in digital holography," *Light Science & Applications*, p. 7, 2018.
- [11] Z. Gang, Z. Zhixiong, W. Huarui, and Y. Yan, "Near real-time digital holographic microscope based on GPU parallel computing," in *Proceedings of the SPIE- 2017 International Conference on Optical Instruments and Technology: Optical Systems and Modern Optoelectronic Instruments*, p. 10616, 2018.
- [12] Z. Zhao, "A holographic display method combing amplitude of real picture and phase of hologram," *Pro. SPIE*, vol. 10255, Article ID 1025503, 2017.
- [13] J. Kühn, J. Conchello, C. J. Cogswell et al., "Real-time dual-wavelength digital holographic microscopy for extended measurement range with enhanced axial resolution," *Biomedical Optics International Society for Optics and Photonics*, 2008.
- [14] Z. Gao, Z. Jiang, Y. Wang et al., "Phase imaging for photorefractive holographic gratings with dual-wavelength digital holography," in *Proceedings of the Photonics Asia*, p. 85561G, Beijing, China.
- [15] Y. Zeng, F. Wang, H. Lei, X. Hu, and X. Hu, "Surface profile measurement of microstructures based on dual-wavelength digital microscopic image-plane holography," *Guangxue Xuebao/Acta Optica Sinica*, vol. 33, no. 10, 2013.

- [16] C. J. Mann, P. R. Bingham, V. C. Paquit, and K. W. Tobin, "Quantitative phase imaging by three-wavelength digital holography," *Optics Express*, vol. 16, no. 13, pp. 9753–9764, 2008.
- [17] S. Peiyong, *3D Topography Recovery of Objects Based on Digital Holographic Technology*, Nanjing Normal University, 2011.
- [18] D. Parshall and M. K. Kim, "Digital holographic microscopy with dual-wavelength phase unwrapping," *Applied Optics*, vol. 45, no. 3, pp. 451–459, 2006.
- [19] A. Khmaladze, M. Kim, and C.-M. Lo, "Phase imaging of cells by simultaneous dual-wavelength reflection digital holography," *Optics Express*, vol. 16, no. 15, pp. 10900–10911, 2008.
- [20] Y. Kou, E. Li, J. Di, Y. Zhang, M. Li, and J. Zhao, "Surface morphology measurement of tiny object based on dual-wavelength digital holography," *Zhongguo Jiguang*, vol. 41, no. 2, 2014.
- [21] D. G. Abdelsalam and D. Kim, "Two-wavelength in-line phase-shifting interferometry based on polarizing separation for accurate surface profiling," *Applied Optics*, vol. 50, no. 33, pp. 6153–6161, 2011.
- [22] W. Yunxin, W. Dayong, Y. Yishu et al., "Application and Analysis in the Biomedicine Field Using Digital Holographic Technology," *Chinese Journal of Lasers*, vol. 41, no. 2, Article ID 002, 2014.
- [23] A. Khmaladze, E. Seeley, J. Jasensky et al., "Dual wavelength digital holographic imaging of cells with phase background subtraction," 2012.
- [24] D. G. Abdelsalam, R. Magnusson, and D. Kim, "Single-shot, dual-wavelength digital holography based on polarizing separation," *Applied Optics*, vol. 50, no. 19, pp. 3360–3368, 2011.
- [25] S. Grare, S. Coetmellec, D. Allano, G. Grehan, M. Brunel, and D. Lebrun, "Dual wavelength digital holography for 3D particle image velocimetry," *Journal of the European Optical Society: Rapid Publications*, vol. 10, no. 3, 2015.
- [26] Z. Yanan, L. Junshen, L. Yuan et al., "Three-Dimensional Displacement Tracking Technique of Particle Based on Digital Holographic Microscopy," *Chinese Journal of Lasers*, pp. 44–12, 2017.
- [27] B. Rappaz, P. Marquet, E. Cuche, Y. Emery, C. Depeursinge, and P. J. Magistretti, "Measurement of the integral refractive index and dynamic cell morphometry of living cells with digital holographic microscopy," *Optics Express*, vol. 13, no. 23, pp. 9361–9373, 2005.
- [28] D. Boss, P. T. So, E. Beaufort et al., "Dual-wavelength Digital Holography for quantification of cell volume and integral refractive index (RI)," in *Proceedings of the European Conferences on Biomedical Optics*, p. 808608, Munich, Germany.
- [29] M. Frómata, G. Moreno, J. Ricardo et al., "Optimized setup for integral refractive index direct determination applying digital holographic microscopy by reflection and transmission," *Optics Communications*, vol. 387, pp. 252–256, 2017.
- [30] Z. Yanan, L. Hai, L. Yuan et al., "Compensation of the Phase Aberrations in Digital Holographic Microscopy Based on Reference Lens Method," *Acta Photonica Sinica*, vol. 47, no. 1, pp. 216–222, 2018.
- [31] Y. Lu, X. Wang, and X. Zhang, "Weighted least-squares phase unwrapping algorithm based on derivative variance correlation map," *Optik - International Journal for Light and Electron Optics*, vol. 118, no. 2, pp. 62–66, 2007.
- [32] S. Li, W. Chen, and X. Su, "Reliability-guided phase unwrapping in wavelet-transform profilometry," *Applied Optics*, vol. 47, no. 18, pp. 3369–3377, 2008.
- [33] Z. Wenjing, X. Qiangsheng, and Y. Yingjie, "Compensation for the Quadratic Phase Aberration in Off-axis Digital Microholography," *Acta Photonica Sinica*, vol. 38, no. 8, pp. 1972–1976, 2009.
- [34] Z. Wang, Y. Chen, and Z. Jiang, "Dual-wavelength digital holographic phase reconstruction based on a polarization multiplexing configuration," *Chinese Optics Letters*, vol. 14, no. 1, pp. 31–35, 2016.
- [35] S. Liu, "Dynamic phase-contrast microscopy of living cells by digital holography," *Journal of Beijing University of Aeronautics & Astronautics*, vol. 38, no. 9, pp. 1186–1188, 2012.



